PALEOMAGNETISM AND TECTONIC INTERPRETATIONS OF THE TAOS PLATEAU VOLCANIC FIELD, RIO GRANDE RIFT, NEW MEXICO

by

Laurie L. Brown, Nancy M. Caffall[1]
Department of Geology and Geography
University of Massachusetts
Amherst, Massachusetts 01003

and

Matthew P. Golombek
Earth and Space Sciences Division
Jet Propulsion Laboratory
Mail Stop 183-50
California institute of Technology
Pasadena, California 91109

Submitted to JGR, 1/93
Revised copy submitted, 6/93

[1] Now at Dept. of Env. Protection, 436 Dwight Street, Springfield, MA 01103

ABSTRACT

The tectonic response of the Taos Plateau volcanic field in the southern San Luis basin to the late stage extensional environment of the Rio Grande rift was investigated using paleomagnetic techniques. Sixty-two sites (533 samples) of Pliocene volcanic units were collected covering four major rock types with ages of 4.7 to 1.8 Ma. Twenty-two of these sites were from stratigraphic sections of the lower, middle and upper Servilleta Basalt collected in the Rio Grande gorge at two locations 19 km apart. Flows from the lower and middle members in the southern gorge record reversed polarities while those in Garapata Canyon are normal with an excursion event in the middle of the sequence. The uppermost flows of the upper member at both sites display normal directions. Although these sections correlate chemically, they seem to represent different magnetic time periods during the Gilbert Reversed-Polarity Chron. Alternating field demagnetization, aided by principal component analysis, yields 55 sites with stable directions representing both normal and reversed polarities, and five sites indicating transitional fields. Mean direction of the normal and inverted reversed sites is I=49.3° and 1X356.7* (a_{95}=3.6°). Angular dispersion of the virtual geomagnetic polesis=16.3°, which is consistent with paleosecular variation model G, fit to data from the past 5 my. Comparison with the expected direction indicates no azimuthal rotation of the Taos Plateau volcanic field; inclination flattening for the southern part of the plateau is 8.3° ± 5.3°. Previous paleomagnetic data indicate 10-15° counter-clockwise rotation of the Espanola block to the south over the past 5 my. The data suggest the Taos Plateau volcanic field, showing no rotation and some flattening in the south and east, has acted as a stable buttress and has been downwarped by overriding of the southeastern end of the plateau by the Picuris Mountains, which makeup the northern corner of the counterclockwise rotat ing Espanola block,

INJ'ROI)IJ(U'1ON

Previous structural and paleomagnetic work has identified a large diamond-shaped block in the north-central Rio Grande rift that has undergone significant counterclockwise rotation (Muehlberger, 1979; Dungan et al., 1984; Brown and Golombek, 1985; 1986; Aldrich, 1986). The block extends from the San Luis basin in the north to the Albuquerque basin in the south and includes the eastern part of the intervening Espanola basin (Figure 1), It is bounded by the following recently active major fault zones: the Embudo fault to the north (Muehlberger, 1979; Dungan et al., 1984; Aldrich and Dethier, 1990), the Pajarito fault zone to the west (Golombek, 1983), the Picuris-Pecos fault to the cast (Montgomery, 1953; Miller et al., 1963) and the Tijeras-Canoncito fault zone to the south (Lisenbee et al., 1979). Extensive structural and paleomagnetic work on the timing and structural con.sequences of counterclockwise block rotation (discussed more fully in Brown and Golombek, 1986) support motion beginning at about 5 Ma that resulted in uplift of the acute corners (Picuris and Sandia uplifts) and subsidence of the obtuse comers (Velarde graben and Santa Fe embayment). Counterclockwise rotation of crustal blocks could be driven by left slip along the rift, which has been suggested previously (Kelley, 1979; 1982; Muehlberger, 1979; Dungan et al., 1984).

The Taos Plateau volcanic field (TPVF) lies within the southern portion of the San Luis basin in the northern Rio Grande rift (Figure 1), north of the proposed rotated block. The San Luis basin is the northernmost of three north-trending, right-echelon, asymmetric, fault-bounded basins that makeup the central Rio Grande rift. The basin is bounded on the cast and the west by the Precambrian-cored Sangre de Cristo and Tusas mountains, respectivel y. It is separated from the Espanola basin on the south by a Precambrian basement high (Manley, 1979) and the Embudo fault along which the Picuris Mountains have been uplifted in the past 5 my. (Muehlberger, 1979; Dungan et al., 1984). Within

the southern San Luis basin is the Taos graben, along which most of the recent activity has been concentrated (Lipman and Mehnert, 1979). It is bounded on the east by the range-bounding fault at the front of the Sangre de Cristo Mountains (estimated to have had 7-8 km of displacement) and on the west by an east-dipping normal fault inferred to be beneath the Rio Grande. A horst abuts the Taos graben on the west exposing early Miocene intrusives, intermediate composition volcanic and pyroclastic rocks attributed to pre-rift (prior to 26 Ma, Hagstrum and Lipman, 1986) and early rift phases of volcanism (Lipman and Mehnert, 1979; Dungan et al., 1984; Thompson et al., 1986).

The TPVF (Figure 2) includes the Servilleta Basalt (olivine tholeiite), and lesser amounts of basaltic andesite, andesite, dacite and rhyolite that were erupted from about 5 to 1.5 Ma (Lipman and Mehnert, 1979; Dungan et al., 1984). A unified magmatic system is suggested by the spatial relationship to basaltic shields on the west margin of the TPVF surrounded, in turn, by andesite and dacite (Lipman and Mehnert, 1979; Figure 2). The lower, middle and upper Servilleta Basalts (LSBs, MSBs and USBs) have been recognized on the basis of field relationships and chemical characteristics and were deposited in short pulses separated by long hiatuses (Dungan et al., 1984; 1986).

In this paper we report on paleomagnetic data from the TPVF in order to answer the following questions. Has the TPVF undergone rotation, and if not, has it been a stable buttress? Has the TPVF undergone warping from the compression and uplift of the Picuris Mountains? In addition, the stratigraphic and geochemical work of Lipman and Mehnert (1979) and Dungan et al. (1984; 1986) in the TPVF makes it possible to investigate correlations between rock type, age and magnetic polarity directions and to integrate these with magnetic reversals and K-Ar ages.

PALEOMAGNETIC TECHNIQUES AND RESULTS

Sixty-two sites were collected to sample the full spatial, temporal, and compositional diversity of the TPVF (Figure 2), with each site representing one unique lava flow. Forty sites on the surface of the plateau were sampled, where possible at sites with published K-Ar age dates (Lipman and Mehnert, 1979; Baldridge et al., 1980; Ozima et al., 1967). Twelve flows in the southern Rio Grande gorge (sites 4051) and ten flows in Garapata Canyon (sites 52-59) were collected in stratigraphic sequence; these correspond to sections 4 and 10 of the Servilleta Basalt sequences of Dungan et al. (1984). Five to 14 samples (average 8) were taken at each flow using a gas-powered rock drill (Doell and Cox, 1967). Samples orientations were determined with both magnetic and sun compasses. Although azimuthal directions were very similar from both methods, the sun compass derived azimuths were used in all cases.

Cores 2.4 cm in diameter were cut to lengths of 2,4 cm for laboratory analysis. Natural remanent magnetizations (NRM) were measured for onespecimen from each core using a Molspin Mini sPin magnetometer; stepwise alternating field demagnetization was done using a single-axis Schonstedt demagnetizer. Thermal studies, using a non-inductivel y wound furnace, were done on selected specimens cut from the same cores that had been stepwise demagnetized using alternating fields.

The Servilleta Basalt (SB) samples from flows exposed in the Rio Grande gorge have NRM intensities of approximately 1 A/m and NRM directions that are well grouped for each site. The samples exhibit stable behavior and directions change only slightly, with improved clustering, after alternating field demagnetization, Median destructive fields are from 40 mT to 80 mT. Typical vector end-point diagrams for cores from both a reversed flow (42TP-326) and a normal flow (50TP-388) show removal of a small overprint and them linear decay to the origin (Figure 3a,b). Samples from two ftows in the southern

gorge (49 and 51) show initial large within-site scatter, indicative of lightning strikes. After extensive demagnetization and the use of principal component analysis (Kirschvink, 1980) samples from both sites provided reliable data.

The samples from flows exposed on the surface of the TPVF (including Servilleta Basalt, andesite and dacite) show NRM directions that are scattered within each site, Initial intensities vary greatly, both within a single flow and between flows, with site mean NRM intensities ranging from a few A/m to greater than 100 A/m. Individual samples show large intensity loss and direction change at low levels of demagnetization (Figure 4a). In some cases stable directions are reached after demagnetization of 30 or 40 mT (Figure 4b), while in other cases stable directions have not been identified after demagnetization to 80 mT. Data for cores from the same site displayed a tendency to converge from widely scattered NRM directions toward a common direction; demagnetization circles were often needed on single samples and on groups of samples from the same ftow to identify characteristic directions, Such behavior was seen in both normal and reversed polarity sites, and in samples from all the represented rock types. This is similar to the behavior of rocks struck by lightning (a distinct possibility on a high plateau in the desert Southwest), but not all samples exhibited the high intensities usuall y linked to lightning strikes.

Samples from four SB flows (sites 54-55B) in Garapata Canyon (part of a magnetic excursion sequence discussed later) demonstrate different magnetic behavior from the other SB samples. Intensities are an order of magnitude less than other gorge flows, and NRM directions show greater scatter. Mean coercivities are variable, but high (Figure 5a), and large direction changes occur during demagnetization (Figure 5b). Samples from all four sites yield transitional directions after demagnetization and, in same cases, application of remagnetization circles.

Of the total 62 sites sampled, 2 sites were excluded from further consideration due to large ($a_{95} > 20°$) within-site scatter after extensive magnetic cleaning. Thermal demagnetization of selected cores from the entire data set confirms the trends and directions

seen on AF demagnetizat ion, but does not aid in identifying primary directions in the scattered sites. None of the site data arc corrected for regional tilt, given that the Servilleta Basalt shows only a negligible eastward dip of 0.4° (Lipman and Mehnert, 1979; Dungan et al., 1984).

Mean magnetic directions of the 60 sites that gave stable directions arc plotted in Figure 6, with site data and statistics given in Table 1. Sites 54,55, 55A, 55B and 15 have intermediate directions and are not included in the calculations of the mean TPVF direction. The mean directions of the different rock types arc all similar at the 95% confidence level, although the small number of sites for all but the Servilleta Basalt result in large confidence limits. Data from reversed sites are inverted to calculate the mean which is I=49.3°, D=356.7° and a_{95}=3.6° (Figure 7). Ten of the eleven flows reported by Ozima et al, (1%7) from the Dunn Bridge site (in the Rio Grande gorge northwest of Taos) yield a mean direction of I=48.5° and D=354.7°, with a_{95}=7.4°. The mean directions from this study are similar to expected directions (I=53.4° and D=357.3°) calculated for this latitude from a mean pole for North America in the late Tertiary, determined by Brown and Golombek (1985), As suggested by Miocene data from the High LavaPlains of Oregon and the Columbia River Basalts (Mankinen et al., 1987), the geocentric axial dipole can be used as a reference field for rocks this young. Por the latitude of the Taos Plateau an inclination of 56.4" and declination of O" is indicated, also in good agreement with the observed data.

REVERSALS AND HXCURSIONS

Correlations of Volcanic Units

Correlations were made between the magnetic directions of Servilleta Basalt sections in the Rio Grande gorge and field and geochemically defined stratigraphic sequences (Dungan et al., 1984). "l'he southern gorge location of this study (sites 40-51, Figure 2; "Southern Gorge", Figure 8) coincides with "section 4" of Dungan et al. (1984). The Garapata Canyon location (sites 52-59, Figure 2; Figure 8) is identical to their section 10. The Dunn Bridge site (Ozima et al., 1967; OZ in Figure 2) is located midway between these two locations. Figure 8 is a compilation of data illustrating Servilleta basalt stratigraphy (Dungan et al., 1984), magnetic polarities (this study; Ozima et al., 1967) and K-Ar radiometric dates (Ozima et al., 1967; Mankinen and Dalrymple, 1979). An attempt was made to quantitatively correlate magnetic directions in these flows using the technique of Bogue and Coe (1981). Although a few individual flows, which already had identical directions, did correlated with this method, the entire sequences proved to be unreliable. This was due not to the fact that the directions arc actually different, but rather to the fact that large within site variances made the statistics inconclusive. As a result, the correlations discussed here are based entirely on polarity.

In the southern gorge section, Dungan et al. (1984) have identified the three packages (I .SB, MSB, and USB) using geochemistry and stratigraphic locations. All paleomagnetic sites in the lower and middle part of the section, as well as the lowermost USB have reversed polarity. The upper part of the USBs, representing the top of the gorge sections and flows covering the nearby plateau, yield normal polarities (Figure 8).

The sequence in Garapata Canyon reveals strikingl y dissimilar magnetic directions from the predominantly reversed section at the southern gorge. Using geochemcial data Dungan

et al (1984) identified the lower most part of the section to be LSB, with a small sequence (three flows) of MSB above. The section then contains a large sedimentary unit, followed by only one USB flow capping the sequence. The lowermost two flows in the section are normal, followed by *4 flows* with transitional directions. The three overlying flows of the MSBs are. again all normal polarity, as is the top flow.

The polarity data from Dunn Bridge (Ozima et al., 1%7) correlate with the results from the southern gorge section. The same reversed polarity for flows in the lower and middle part of the section is seen, with the only normal polarities observed at the top of the section (Figure *8).* There is some uncertainty and confusion concerning the specific sampling locations at Dunn Bridge and their relationship to a fault (down to the west) which intersects the gorge a t Dunn Bridge. "l"his, with the lack of geochemcial data on this section, makes direct correlation between polarities and stratigraphy difficult.

Although our southern gorge data agree with the Dunn Bridge data (Ozima et al., 1967), the I .SBs and MSBs with reversed polarities at both these localities do not correlate with the normal and transitional directions at Garapata Canyon. This discrepancy could be due to the fact that lava ftows do not represent an uninterrupted, continuous record of the earth's magnetic field. Or, the flow units in the Taos plateau could be much more restricted in areal extent than previously thought, and these sections sample lava packages separate in space and time.

Potassium-argon dates for samples from the Servilleta Basalt in and near the Rio Grande gorge (Ozima et al., 1967, corrected using Dalrymple, 1979; Mankinen and Dalrymple, 1979; Baldridge et al., 1980) range from 4.67 to 3.72 Ma. This suggests an emplacement time for the entire central Rio Grande gorge sequence of roughly 1.0 my. The dates fall within the Gilbert Reversed-Polarity Chron, a period of predominantly reversed polarity with numerous subchrons of normal polarity (Mankinen and Dalrymple, 1979). Dungan et al. (1984) suggest that the flow packages were deposited in spurts of several hundred years duration with much longer periods of inactivity in between based on geochemical

similarities and thicknesses of interbedded sediments. Therefore, large portions of the magnetic polarity time scale may not have been recorded by the Servilleta Basalt, and although some flows correlate chemicall y, they may represent different polarity intervals.

Garapata Canyon Excursion

The transitional directions of the four 1 .SB flows in Garapata Canyon describe an excursion of the magnetic field. Sites 52 and 56, below and above the transitional sites, arc both normal and behave as typical SBs with little change in direction during demagnetization. The transitional flows have lower intensities (by an order of magnitude) and relativel y complex demagnetization curves (Figure 5b). The high median destructive fields (Figure 5a), linear decay of the demagnetization vector end-points, and within-site stability indicate that the component isolated above 20 m'T' demagnetization is a stable primary direction,

The inclinations and declinations for the Garapata Canyon sites (flows 52-58, Figure 8) are listed in Table 1. The lowermost flows (and lowest flows exposed in this area) have normal polarities. Continuing along a great circle path and stratigraphically up section, there is an increase in declination, a shallowing of inclination and a decrease in intensity. As the excursion proceeds, there is a return to normal polarity along a great circle path at steeper inclinations and an increase in intensities to the original levels. Flows 57 and 58 arc separated from the transition flows by a thin soil horizon, but they lie directly along the great circle path of the return to normal polarity and arc, therefore, considered to be part of the excursion. This can be seen in Figure 9a where the Garapata Canyon section data are projected down the mean axial dipole field direction for the site latitude (e.g. Hoffman, 1984). The data describe a well defined excursion with a slight degree of near-sidedness. Figure 9b, a global projection of the virtual geomagnetic poles (VGPs) of the Garapata excursion, shows the largest departure of VGPS from geographic north is reached at

latitude 22° south and longitude 320° east, on the cast coast of South America. It is intersting to note that this location conicides with one of two global "cluster patches" of transitional directions identified by Hoffman (1992). Data from both complete reversals and excursions show a preference for these positions, indicating the possible influence of the lower mantle on the core dynamo (Hoffman, 1992). General correlation to the dates from Dunn Bridge (Ozima et al., 1967) places the excursion observed herein the Gilbert Chron, but further refinement of age is not possible with the available data.

inclination Anomaly and Paleosecular Variation

Using the mean inclination (49.3°) for the TPVF, an inclination anomaly (dI) of -6.7° is obtained between the observed inclination and the inclination expected from the geocentric axial dipole. Late Quaternary studies at similar latitude from California and Tennessee yield dI values of -5.5° and -3.9°, respectively (1 rend, 1985). These data points agree at the 95% level with worldwide averaged results for the past 5 my. by Lee (1983, as reported in Merrill and McElhinny, 1983). This analysis distinguished between normal and reversed polarity information; if only normal sites from the TPVF are used, a dI of -10,7° is obtained, which is statistically significant from the global data. Only a very small part of this low value is possibly due to tectonic tilting in the southern part of the plateau (see discussion below), because normal sites predominate in the northern part of the sampling area, where little or no shallowing has occurred.

Angular dispersion of the VGPS of the TPVF, excluding the 5 excursion sites, was calculated using standard methods. As reported in Table 2, the angular standard deviation for the TPVF, calcualted with respect to the geographic axis, is 16.3°, with upper and lower 95% errors of 18.9° and 14.4°, respectively (Cox, 1969). This observed VGP scatter is similar to that predicted by the most recent model comparing secular variation to latitude. Model G (McFadden et al., 1988) provides a variation of VGP scatter with

respect to latitude dependent on the contributions of the dipole and quadruple families. This curve is shown in Figure 10 fit to averaged global data for the past 5 m.y.(McFadden et al., 1988) along with the VGP dispersion for the Taos data. Other published angular standard deviations for areas in North America at similar latitudes are given in Table 2. These include anomalously low paleosecular variation recorded for the western United States (Doell and Cox, 1972; WUS1, Table 2) and Anderson Pond, Tennessee (J .und, 1985; APT, Table 2), but both these studies deal only with late Quarternary data. Data on lava flows in eastern Arizona younger than 2.1 Ma yield a dispersion of 18.0° (Castro *et* al., 1985; AZ, Table 2), greater than expected from the model.. A compilation of western United States data spanning the last 5 my. (McElhinny and Merrill, 1975; WUS2, Table 2) yields an angular dispersion in c1osc agreement with that predicted by model G.

The observations that dI is low, but paleosecular variation for the TPVF is as expected, is not inconsistent. As noted by 1.und (1985), these two phenomena do not have to be generated by the same processes, and can bc considered independent. It is also well known that "spot" readings of the magnetic field, as represented by dI or paleosecular variation, may be spurious (Merrill and McElhinny, 1983). However, consistent data over a regional area and averaged over millions of years suggests that variations of the non-dipole field may be much more complex than presently supposed (Brown and Castro, 1987).

TECTONIC ROTATIONS

In an effort to investigate the tectonic behavior of the southern San Luis basin during the last 5 my. mean inclination and declination for the TPVF were each compared to the expected inclination and declination. Changes in declination from the expected declination can be viewed as rotations (horizontal movements around a vertical axis). Flattening,

changes in the inclination compared to the expected inclination, represent a north-south translation (Beck, 1980), or tilt around a horizontal axis.

Using a North American reference pole for the late Tertiary determined by Brown and Golombek (1985) and methods of Beck (1980) and Demarest (1983), the rotation and flattening have been calculated ('Table 3). The 55 non-excursion sites of the TPVF yield a rotation of 0.6° ± 5.6° and a flattening of 4. 1°± 4.10. These data indicate no rotation of the TPVF; although to the south, the Espanola and Jemez blocks may have been rotated approximately 15° counterclockwise and clockwise, respectively (Brown and Golombek, 1985; 1986).

Considering all of the TPVF data, there is a small amount of flattening (4.1° ± 4. 1°), but it is not statistically significant.. To test whether flattening is observable in localized regions, the data were subdivided into geographic areas (north, mid and south TPVF; east and west TPVF). This grouping was also done to test the hypothesis of bowing of the TPVF or downwarping of the southern plateau as proposed by Muehlberger (1 979) and Dungan et al. (1984) due to recent NW-SE compassion from the overriding of the Picuris Mountains at the plateau's southeast corner. If there has been recent (less than 5 Ma) arching of the plateau, the geometry of the magnetic directions, in relation to the tilting, would require that the inclinations at sites on the northwest limb of an arch with a NE-trending fold axis would steepen, and the inclinations on the southeast limb would become more shallow (e.g. Figure 11). Although the error bars on the flattening of the northern and mid TPVF would indicate these are not significant, there is a definite trend from north to south (Table 3).. The northern group have steepened slightly (-0.4° ± 6.20), the mid TPVF group reflect the mean flattening (4.2° ± 6.20), and the southern group is shallower than the mean, with a statistically significant flattening of 8.3° ± 5.3°. A similar pattern of tilting is seen in an east-west comparison, with the eastern half of the area indicating some downwarping (flattening of 5.7° ± 4.6°) and negligible tilt in the western half. These data support the suggestion that the TPVF has acted as a stable buttress against which the

Espanola block to its south has rotated. As a result, the Picuris Mountains, which comprise the Espanola block's northeast comer, have been thrust up and over the TPVF, thereby downwarping the plateau at its southern end. It appears that for this compression to occur, the rate of extension across the southern Taos graben, the recently active sub-basin of the San Luis basin, must be less that the rate of rotation or westward translation of the northern comer of the Espanola block. If the rate of rotation or western translation of the northern Espanola block were less than the extension in the southern San Luis basin near the Embudo fault, no compression and uplift would occur. Evidence suggests some compression across the southwestern Embudo fault (Aldrich, 1986), which could be due to convergence from the clockwise rotation (Figure 11) of the Jemez block (Brown and Golombek, 1985); it is not clear if the southwestern comer of the Taos Plateau and/or Tusas Mountains have been similarly compressed.

The warping and lack of rotation of the TPVF show that it has acted as a stable buttress to the rotation of the Espanola block to the south. The reason for rotation of crustal blocks to the south, but not in the San Luis basin is not known, although we can speculate on contributing factors. The long axis of the diamond-shaped Espanola block strikes NE and its bounding faults strike NE and NNE, which are at a slight angle from perpendicular to the least principal horizontal stress (E-W) that has existed throughout the region for at least the past 5 my. (Zoback and Zoback, 1989; Lipman, 1981; Zoback et al., 1981; Golombek et al., 1983; Aldrich et al., 1986). This oblique geometry could result in a component of left slip along the Espanola block that could drive its observed counterclockwise rotation. In contrast, the recently active portion of the southern San Luis basin (Taos graben) is bounded by faults that strike more nearly due north, perpendicular to the least principal horizontal stress (no component of strike slip), and so does not rotate. In addition, if Kelley's model of north-shallowing basins that step to the right along en echelon relay faults is correct, it could also contribute to the left slip (e.g., Kelley, 1979; 1982), Finally, it is interesting to note that the clockwise rotated Jemez block (adjacent to the Colorado

Plateau) lies in a different least principal horizontal stress field that is oriented predominantly NW-SE (Aldrich et al., 1986), which could result in the clockwise rotation as originally suggested by Golombek et al. (1983) and elaborated upon by Brown and Golombek (1985).

SUMMARY AND CONCLUSIONS

1. 533 samples were collected sixty-two sites in the Servilleta Basalt, basaltic andesite, andesite, dacite, and rhyolite of the Taos Plateau volcanic field. Samples from sixty sites yielded stable directions, and 55 were used to calculate a mean direction for the TPVF of I=49.3° and D=356.7° (a_{95}=3.6°).

2. Demagnetization behavior of samples from sites in the Rio Grande gorge and normal polarity sites on the surface of the plateau is straightforward, with simple linear decay to the origin. Reversed polarity samples from sites on the plateau surface show some overprinting and considerably more scatter after demagnetization than the normal sites. Samples from sites representing an excursion of the magnetic field show low intensities and more complex demagnetization paths.

3. The magnetic directions of 4.7 to 3.6 Ma Servilleta basalts in the Rio Grande gorge reflect normal, intermediate, and reversed polarities within the Gilbert Chron. The magnetostratigraphy of flows in the southern gorge, Dunn Bridge, and Garapata Canyon localities do not cm-elate, even though their geochemistry indicates similar packages of flows. One explanation for thi is that the flows were implaced in short time periods (several hundreds of years) with longer intervals between eruptive events, and thus reflect different magnetic polarity time periods.

4. Data for nine basalt flows in Garapata Canyon reflect an excursion of the magnetic field during a period of normal polarity. The fullest extent of the excursion is marked by a virtual geomagnetic pole at 22° south latitude and shows a slight degree of near-sidedness.

5. The inclination anomaly for the TPVF is -6.7°, agreeing with global data averaged over the last 5.0 m. y. The angular di spcrsion of virtual geomagnetic poles from the TPVF is 16.3°, similar to expected val ucs from the current model for palcosecular variation,

6. Although rocks to the immediate south have been rotated both clockwise (Jemez block) and counterclockwise (Espanola block), the paleomagnetic data for the TPVF indicate no sign of rotation. (R= 0.6°3 5.60). It is suggested that the TPVF has acted as a stable buttress to the crustal blocks to the south.

7. The flattening of the magnetic inclinations in the TPVF is statistically insignificant (4. 103 4.10), but separation of the data reveals significant flattening in the southern (8.3° ± 5.7°) and eastern (5.7° ± 4.6°) parts of the plateau. This finding agrees with downwarping and bowing of the TPVF due to NW-SE compressional stresses created by the overriding of the Picuris Mountains to the southeast. It also supports the concept of the southern San Luis basin and TPVF as a stable buttress and requires that the rate of extension across the southern Taos graben and San Luis basin be less than the rotation and westward translation of the northern corner of the Espanola block.

Acknowledgments. Field work was generousl y supported by the New Mexico Bureau of Mines and Mineral Resources. Field assistance provided by C. Condit and I. Brown. Special thanks to M.A. Dungan for his help and enthusiasm, and to Southern Methodist Universit y for hospitality at their Fort Burgwin Research Center. Reviews by M.J. Aldrich, Jr., E. Mankinen, and associate editor J. Geissman were most helpful. MPG supported by National Aeronautics and Space Administration contracts to the Jet Propulsion 1 aboratory, California Institute of Technology.

REFERENCES

Aldrich, M. J., Jr., Tectonics of the Jemez lineament in the Jemez Mountains and Rio Grande rift, *J. Geophys. Res., 91*, 1753-1762, 1986.

Aldrich, M. J., Jr., C. E. Chapin, and A.W. Laughlin, Stress history and tectonic development of the Rio Grande rift, *J. Geophys. Res.*, 91, 6199-6211, 1986.

Aldrich, M. J., Jr., and D.P. Dethier, Stratigraphic and tectonic evolution of the northern Espanola basin, Rio Grande rift, New Mexico, *Geol. Soc. Amer. Bull.*, 102, 1695-1705, 1990.

Baldridge, W. S., P. R. Damon, M. Shafiqullah, and R.J. Bridwell, Evolution of the central Rio Grande rift, New Mexico; New potassium-argon ages, *Earth Planet. Sci. Lett.*, 51, 309-321, 1980.

Beck, M.E., Jr., Paleomagnetic record of plate-margin tectonic processes along the western edge of North America, *J. Geophys, Res.*, 85, 7115-7131, 1980.

Bogue, S.W. and R.S. Cot, Paleomagnetic correlation of Columbia River Basalt flows using secular variation, *J. Geophys. Res.*, 86, 11,883-11,897, 1981.

Brown, L.L. and J. Castro, Paleosecular variation for western North America: Regional data in time and space (abstract), *Int. Union Geod. Geophys., X1X Gen. Assem.*, 2, 477, 1987.

Brown, L.L. and M.P. Golombek, Tectonic rotations within the Rio Grande rift: Evidence from paleomagnetic studies, *J. Geophys. Res.*, *90*, 790-802, 1985.

Brown, 1,,1,. and M.P. Golombek, Block rotations in the Rio Grande rift, *Tectonics, 5, 423-438, 1986.*

Castro, J., 1.. Brown, and C. Condit, Secular variation in southwestern United States Data from the Springerville volcanic field, Arizona (abstract), Trans. *Amer. Geophys. Union,* 66, 879, 1985.

Cox, A., Confidence limits for the precision parameter k, Geophys, *J. Roy. Astron. Sot.,* 18,545-549,"1969.

Dalrymple, G.B., Critical tables for conversion of K-Ar ages from old to new constants, *Geology,* 7,558-560,1979.

Demarest, H.H., Jr., Error analysis for the determination of tectonic rotation from paleomagnetic data, *J. Geophys. Res.*, 88,4321-4328, 1983.

Doell, R.R., and A. Cox, Paleomagnetic sampling with a portable coring drill, in Methods ': *in Paleomagnetism*, ed. by D.W. Collinson, K.M. Creer, and S.K. Runcorn, pp. 21-25, Elsevier, Amsterdam, 1967.

Doell, R.R. and 'A. Cox, The Pacific geomagnetic secular variation anomaly and the' question of lateral uniformity in the lower mantle, in *Nature of the Solid Earth,* ed. by E.C. Robertson, pp. 245-284, McGraw-Hill, New York, 1972.

Dungan, M. A., M.M. Lindstrom, N.J. McMillan, S. Moorbath, J. Hocfs, and L.A. Haskin, Open system magmatic evolution of the Taos Plateau volcanic field, northern New Mexico 1. The petrology and geochemistry of the Servilleta Basalt, *J. Geophys, Res.*, 91, 5999-6028, 1986.

Dungan, M. A., W.R. Muehlberger, L. Leininger, C. Peterson, N.J. McMillan, G. Gunns, M. Lindstrom, and 1.. Haskin, Volcanic and sedimentary stratigraphy of the Rio Grande gorge and the late Cenozoic geologic evolution of the southern San Luis Valley, *New Mex. Geol.* Sot. *Field Conf. Guidebk., 3.5,* 157-170, 1984.

Fisher, R., Dispersion on a sphere, *Proc. Roy. Sm., Ser. A.,* 217, 295-305, 1953.

Golombek, M.P., Geology, structure and tectonics of the Pajarito fault zone in the Espanola basin of the Rio Grande rift, New Mexico, *Geol.* Sot. *Am. Bull.,* 94, 192-205, 1983.

Golombek, M. P., G. Ii. McGill, and 1..1.. Brown, Tectonic and geologic evolution of the 1 Espanola basin, Rio Grande rift: Struct urc, rate of extension, and relation to the state of stress in the western United States, *Tectonophysics, 94, 483-507, 1983.*

Hagstrum, J. T., and P. W. Lipman, Paleomagneti sm of the structural] y deformed I stir volcanic field, northern Ncw Mexico, Relations to formation of the Questa Caldera and development of the Rio Grande rift, *J. Geophys. Res., 91, 7383-7402, 1986.*

Hoffman, K .A., A method for the display and analysis of transitional paleomagnetic data, *J. Geophys. Res.,* 89, 6285-6292, 1984.

1 Ioffman, K. A., Dipolar reversal states of the geomagnetic field and core-mantle dynamics, *Nature*, *.?.59, 789-794, 1992.*

Kelley, V. C., Tectonics, middle Rio Grande rift, New Mexico, in *Rio Grande Rift: Tectonics and Magmatism, cd,* by R.E. Riecker, pp. 57-70, AGU, Washington, 1979.

Kelley, V. C., The right-relayed Rio Grande rift, Taos to Hatch, Ncw Mexico, *New Mex. Geol.*. Sot. *Field Conf. Guidebk., 3.?,* 14"?-151, 1982.

Kirschvink, J.L., The least-squares line and plane and the analysis of paleomagnetic data, *Geophys. J. Roy. Astron. Sot., 62, 699-718, 1980.*

I ee, S., A study of the time-averaged paleomagnetic field for the last 195 million years, Ph.]>. thesis, Aust. Nat. Univ., Canberra, 357 pp., 1983.

Lipman, P.W., Volcano-tectonic setting of Tertiary ore deposits, southern Rocky Mountains, *Ariz. Geol. Sot. Digest, 14, 199-213, 1981.*

Lipman, P.W. and H.H. Mehnert, The Taos Plateau volcanic field, northern Rio Grande rift, New Mexico, in *Rio Grande Rift: Tectonics and Magmatism, ed.* by R.E. Riecker, pp. 289-312, AGU, Washington, 1979.

Lisenbee, A.] . . . L.A. Woodard, and J.R. Connally, Tijeras-Canoncito fault system - A major zone of recurrent movement in north-central New Mexico, *New Mex. Geol. Sot. Field Conf. Guidebk., 30, 89-100, 1979.*

Lund, S.T., A comparison of the statistical secular variation recorded in some late Quaternary lava flows and sediments, and its implications, *Geophys. Res. Lett., 12, 251-254, 1985.*

Mankinen, E.A., Revised paleomagnetic pole for the Sonoma volcanics, California, *Geophys. Res. Lett., 16, 1081-1084, 1989.*

Mankinen, E.A. and G.B. Dalrymple, Revised geomagnetic polarity time scale for the interval *0-5* m.y.B.P., *J. Geophys. Res., 84, 615-626, 1979.*

Mankinen, E.A., E.E. Larson, C.S. Gromme, M. Prevot and R.S. Cot, The Steens Mountain (Oregon) Geomagnetic Polarity Transition 3. Its Regional Significance, *J. Geophys. Res.,* 92, 8057-8067, 1987.

Manley, K., Stratigraphy and structure of the Espanola basin, Rio Grande rift, New Mexico, in *Rio Grande Rift: Tectonics and Magmatism, cd.* by R. E. Riecker, pp. 77-86, AGU, Washington, 1979.

McElhinny, M.W. and R.T. Merrill, Geomagnetic secular variation over the past 5 my., *Rev. Geophys. Space Phys., l.?,* 687-708, 1975.

McFadden, P.L. and F.J. Lowes, The discrimination of mean directions drawn from Fisher distributions, *Geophys. J. Roy. Astr. Sot., 67, 19-33, 1981.*

McFadden, P.L. and M. W. McElhinny, The combined analysis of demagnetization circles and direct observations in paleomagnetism, *Earth Planet. Sci. Lett.,* 87, 161-172, 1988.

McFadden, P.I . . . Merrill, R.T. and M.W. McElhinny, Dipole/quadrupolc family modeling of paleosecular variation, *J. Geophys. Res.*, *93*, 11,583-11,588, 1988.

Merrill, R.T. and M.W. McElhinny, *The Earth's Magnetic Field: Its History, Origin and Planetary Perspective*, Academic Press, I ondon, 401 pp., 1983.

Miller, J. P., A. Montgomery, and P.K. Sutherland, Geology of part of the southern Sangre de Cristo Mountains, New Mexico, *New Mex. Bur. Mines & Min. Res., Mm. 11*, *106* pp, *1963.*

Montgomery, A., Pre-cambrian geology of the Picuris Range, north-central Ncw Mexico, New *Mex. Bur. Mines& Min. Res.*, Bull. *30, 89* pp., 1953.

Muehlberger, W. R., The Embudo fault between Pilar and Arroyo Hondo, New Mexico: An active intracontinental transform fault, *New Mex. Geol. Soc. Field Conf. Guidebk., 30, 77-82,* 1979.

Onstott, 'l'.C., Application of Bingham distribution function in paleomagnetic studies, *J. Geophys. Res., 85, 1500-1510, 1980.*

Ozima, M., M. Kono, 1. Kaneoka, H. Kinoshita, 'J'. Nagata, E.E. 1 arson, and D.W. Strangway, Paleomagnetism and potassium-argon ages of some volcanic rocks from the Rio Grande Gorge, Ncw Mexico, *J. Geophys. Res.*, 72, *2615-2621, 1967.*

Thompson, R. N., M.A. Dungan, and P.W. Lipman, Multiple differentiations processes in early-rift talc-alkaline volcanics, Northern Rio Grande Rift, Ncw Mexico, *J. Geophys. Res.*, *91,* 6046-6058,"1986.

Zoback, M.].. and M. D. Zoback, Tectonic stress field of the continental United States, in Pakiser, 1.. C. and W. D. Mooney, eds., Geophysical framework of the continental United States, *Geol. Sot. Amer. Mem. 172,* 523-539, 1989.

Zoback, M.]... R.E. Anderson, and G.A. Thompson, Cainozoic evolution of the state of stress and style of tectonism of the Basin and Range province of the western United States, *Phil. Trans. R.* Sot. *Lond., A300, 407-434, 1981.*

FIGURE CAPTIONS

Figure 1. Generalized geologic map of the northern Rio Grande rift, New Mexico. The Taos Plateau volcanic field lies within the southern San Luis Basin. Some important faults within the rift are: the Embudo fault, EF; the Pajarito fault zone, PFZ; the Picuris-Pecos fault, P-PF; the Tijeras-Canoncito fault zone, T-CF.

Figure 2. Generalized geologic map of the "lTaos Plateau volcanic field, northern New Mexico. Numbered circles refer to paleomagnetic sites listed in Table 1. Patterns: dashed, Miocene and earlier undifferentiated reeks; dotted, Servilleta Basalt; wavy, andesite; vertical lined, rhyolite; NI i-SW lined, dacite; NW-SE lined, xenocrystic basaltic andesite; plain, Quarternary basin fill. OZ refers to Dunn Bridge location of Ozima et al. (1967). Adapted from Lipman and Mehnert (1979).

Figure 3. Vector end-point diagrams for typical flows of the Servilleta Basalt exposed in the Rio Grande gorge, showing both reversed (a) and normal (b) directions, with simple decay curves and little overprinting. Closed circles are horizontal projections, open circles are vertical projection; numbers are alternat ing field demagnetization levels in m"]'.

Figure 4. Vector end-point diagrams for units exposed on the surface of the Taos Plateau for normal (a) and reversed (b) polarities, both showing viscous behavior below 30 mT. Symbols as in Figure 3.

Figure 5. Demagnetization data on flows of the Garapata Canyon excursion. 5a, normalized intensity plot for four samples, one each from the four excursion flows. 5b, typical vector end-point diagram for sample from the excursion, symbols as in Figure 3.

Data shows high mean destructive fields and considerable direction change during demagnetization.

Figure 6, Stereographic projection of site mean data after demagnetization for TPVF. Open symbols are projections on the upper hemisphere, closed symbols are projections on the lower hemisphere. Circles, assorted units; squares, Servilleta basalts recording excursion.

Figure 7, Portion of stereographic projection comparing the mean direction for the TPVF (asterisk) to the expected direction at this latitude (dot). Tick marks are 20°. Square is mean for 1 Dunn Bridge location of Ozima et al.(1967). All means shown with circles of confidence at the 95 % level.

Figure 8. Stratigraphic and magnetostratigraphic sections of Servilleta Basalts in the Rio Grande gorge. White, lava flows; stippled pattern, sediments and/or rubblezones; dashed pattern, alteration zones; N, normal polarity; R, reversed polarity; USB, MSB, LSB, upper, middle, and lower Servilleta Basalt; numbers refer to paleomagnetic sites listed in 'l'able 1, Southern Gorge and Garapata stratigraphy and Servilleta Basalt correlations from Dungan et al. (1984); Dunn Bridge stratigraphy and polarity from Ozima et al. (1967). Radiometric dates from Ozima et al. (1967), corrected using new decay constants (Dalrymple, 1979).

Figure 9. Stereographic projections of Garapata Canyon excursion. a) plot of inclination and declination, centered on axial dipole direction for site (Hoffman, 1984), open symbols, upper hemisphere; closed symbols, lower hemisphere. b) plot of virtual geomagnetic pole date for excursion, star is mean pole for TPVF data.

Figure 10. Angular dispersion of virtual geomagnetic poles plotted with respect to latitude. Dispersion of poles from the TPVF (triangle) with 95 % confidence limits plotted on secular variation model G of McFadden et al. (1988). Solid line is model G fit to averaged global data 0-5.0 Ma (solid dots).

Figure 11. Schematic diagram of rotated and unrotated blocks in the Rio Grande rift, northern New Mexico. EF, Embudo fault; PFZ, Pajarito fault zone, VG, Velarde Graben. The Jemez block has rotated clockwise, the Espanola block has rotated counterclockwise, and the TPVF shows no rotation in the past 5 my. Counter-clockwise rotation of the Espanola block has caused convergence at its NE corner (Picuris Uplift). This convergence has resulted in NW-SE compression and thrust motion along the end of the Embudo fault, uplift and overriding of the Taos Plateau by the Picuris Mountains, and downwarping of the southern Taos Plateau.

TABLE 1. Magnetic Directions, Taos Plateau Volcanic Field

Site	I at	I ong	N	J_{NRM}	1	D	a_{95}	k	PI A	PI O
Servilleta Basalt										
2	36.78	254.02	2/3/7	1.2	-86.4	199.7	9.]	92	-43.5	77.3
3	36.78	254.02	6/6	15.6	-63.5	178.9	5.9	93	-81.6	67.2
4	36.74	254.02	3/6/10	102.6	42.6	7.6	7.9	49	76.2	43.7
5	36.65	254.04	7/7	21.1	34.6	0.5	6.9	58	72.4	72.5
6	36.65	254.04	7/7	78.9	27.1	351.6	12.8	17	66.5	94.8
7	36.34	253.94	7/7	5.7	-34.3	186.6	7.2	54	-71.6	233.8
8	36.78	254.02	4/3/7	40.0	-64.1	173.2	8.4	58	-79.6	46.8
10	36.82	254.02	3/5/8	69.0	-65.3	177.2	8.2	53	-79.2	63.8
13	36.92	254.01	6/7	18.2	50.6	355.8	6.8	97	83.4	107.1
20	36.76	254.27	2/4/9	26,6	34.1	3.7	8.6	78	71.7	63.1
21	36.35	254.26	8/8	3.4	40.1	3s4. 1	2.3	591	75.6	96.6
22	36.36	254.20	7/7	9.6	38.4	3.6		127	74.9	61.2
23	36.36	254.15	5/3/8	11.0	-62.8	142.2	1 ; :	35	-60.4	11.4
24	36.44	254.09	2/4/7	23.3	-31.2	175.6	8.4	81	-70.0	266.5
25	36.53	254.05	8/1 /9	13.9	57.0	351.8	6.3	69	83.4	175.7
26	36.61	253.98	5/1 /9	43.0	48.6	353.7	12.4	31	82.1	112.6
27	36.75	254.33	6/7	11.4	42.7	352.9	5.6	142	76.6	103.2
29	36.72	254.16	4/3/8	69.5	-20.5	166.5	9.2	64	-61.2	282.6
30	36.62	254.00	2/5/9	61.1	48.2	352.1	7.6	77	80.1	118.2
32	36.57	254.21	7/8	12.3	-44.8	186.1	5.6	119	-78.6	225.5
34	36.51	254.24	9/11	7.6	31.7	355.6	5.6	85	70.3	86.8
35	36.48	254.26	4/2/8	33.4	27.0	358.1	8.8	64	67.7	79.1
40	36.44	254.27	7/7	2.2	-51.0	164.7	3.5	299	-76.5	328.2
41	36.44	254.27	6/6	3.4	-51.1	172.1	3.4	390	-82.0	311.1
42	36.44	254.27	6/7	5.9	-47.2	170.6	2.8	579	-78.7	301.4
43	36.44	254.27	8/8	4.9	-39.8	185.1	7.4	57	-75.5	235.2
44	36.44	254.27	7/7	1.5	-49.7	189.3	3.1	372	-80.3	199.0
45	36.44	254.27	7/7	2.2	-43.0	178.7	3.8	257	-78.5	260.2
46	36.44	254.27	7/7	1.8	-45.7	179.0	4.4	192	-80.7	259.8
47	36.44	254.27	7/7	2.5	-45.7	181,8	3.3	328	-80.6	244.5
48	36.44	254.27	8/8	2.2	-50.8	154.6	2.0	778	-68.4	338.5
49	36.44	254.27	8/8	20.5	-55,9	151.9	(3.3,4.7	-167,-2,)	-66.8	353.0
50	36.44	254.27	8/8	2.2	41.7	357.0	3.6	240	77.3	86.8
51	36.44	254.27	2/4/7	45.1	31.7	355.3	9.2	68	70.3	87.7
52	36.61	254.31	7/7	1.4	43.7	4.4	2.0	937	78.3	54.3
53	36.61	254.31	7/7	3.5	45.7	9.1	2.7	519	77.8	32.6
54*	36.61	254.31	6/7	0.8	16.9	115.8	4.6	217	-14.8	321.3
55*	36.61	254.31	7/7	0.8	10.5	122.5	7.1	73	-22.0	319.2
55A*	36.61	254.31	4/4/8	0.9	15.5	119.7	5.8	102	-18.2	319.2
55B*	36.61	254.31	5/1/7	2.5	60.4	67.6	11.9	34	38.6	316.9
56	36.61	254.31	8/8	3.2	64.3	359.6	1.9	859	80.5	252.6
57	36.61	254.31	6/6	3.4	63.1	11.3	4.4	237	78.3	297.8
58	36.61	254.31	7/7	3.5	65.4	21.5	3.3	341	70.8	303.0
59	36.61	254.31	12/14	22.9	39.5	349.5	4.6	89	73.1	110.3
60	36.28	253.94	5/2/9	21.0	-56.7	204.2	10.9	33	-70.6	153.7
MEAN			41 /45		47.4	357.2	4.2	230	81.7	91.6

Xenocrystic Basaltic Andesite										
11	36.88	254.06	7/8	38.6	-57.1	183.8	9.3	43	-86.9	147.7
12	36.89	254.06	3/4/7	16.9	-53.6	173.0	11.3	33	-83.7	320.4
16	36.83	253.94	1/5/8	109,8	50.8	349.5	6.7	143	79.8	135.5
17	36.82	253.98	6/8	9.6	41.6	10.4	(8.3,10.2	-42,-1)	74.3	36.3
18	36.79	254.01	3/5/8	31.4	-70.6	156.0	8.8	46	-65.6	39.4
19	36.78	254.06	4/2/6	18.7	-57.8	183.1	11.8	36	-87.0	28.9
MEAN			6/6		55.7	357.9	9.6	50	88.3	52.8
Andesite										
14	36.90	254.02	6/2/8	47.2	44.6	354.8	5.0	129	78.5	98.0
15*	36.89	254.03	3/5/9	169.2	-3.9	7.2	10.9	30	-50.6	242.7
33	36.55	254.24	8/8	23.0	-76.2	152.5	7.8	51	-58.1	51.6
36	36.69	254.38	8/8	12..7	55.0	359.2	11.8	23	88.7	103.7
MEAN			3/4		58.9	353.0	26.5	23	83.7	195..3
Dacite										
28	36.72	25433	7/8	37.3	61.3	10.4	(6.3,1	0.0 -5 1,-2)	80.3	295.4
31	36.59	254.16	8/8	4.7	-22.7	161.9	103	30	-60.3	292.1
37	36.58	?,54.83	8/8	1.8	-57.5	166.2	5.2	115	-78.9	356.5
38	36.57	254.82	7/8	2.4	-47.6	175.8	2.9	428	-81.4	279.7
39	36.54	254.83	9/10	1.2	-60.7	176.4	3.0	302	84.1	227.5
MEAN			5/5		50.5	352.3	16.9	22	81.7	12.6.7
TPVF MEAN			55/60		49.3	356.7	3.6	29	83.1	98.9
EXPECTED^					53.4	357.3	3.5		86.5	114.7

Lat and Long, north latitude and east longitude, in degrees, of each site location
N, number of samples (sites) used in calculations: number of samples (sites) measured or, number from direct observations / number from remagnetization circles, / total number measured
J_{NRM}, Mean intensity of all samples measured for NRM, in A/m
I and D, mean inclination, positive downward, and declination, east of north, in degrees
a_{95}, radius of cone of 95% confidence around mean direction
k, precision parameter (Fisher, 1953), precision parameter for mixed sites from McFadden and McElhinny (1988)
(,), parameters for Bingham statistics (Onstott, 1980), determined using remagnetization circles
PLA and 1'1.0, pole latitude, positive northward, and pole longitude, eastward, in degrees

*, transitional directions not included in mean calculations
', expected direction from reference pole of Brown and Golombek (1985), calculated for latitude of TPV1?

Table 2. Paleosecular variation. Western United States

Site	1 at	N	Sf	Su	S1	Age	Ref
AZ	34.0	46	18.0	21.1	15.7	<2.1	6
TPVF	36.5	52	16.3	18.9	14.4	1.8-4.7	1
WUS2	37.0	76	16.3	18.4	14.7	<5.0	3
Alyl'	37.0		11.6	12.8	10.6	<0.02	4
WUS1	38.0	21	12.5	15.9	10.3	<0.7	2
Sv	38.5	25	18.5	23.1	15.4	3-8	5

1 at, degrees north latitude; N, number of sites; Sf, angular dispersion of VGP data, in degrees; Su and S1, upper and lower 95% error limits (Cox, 1969); Age, millions of years; AZ, Springerville Volcanic Field, Arizona, (6), Castro et al., 1985; TPVF, Taos Plateau Volcanic Field, (1) this study; WUS2, Western United States, (3), McElhinny and Merrill, 1975; APT, Anderson Pond, Tennessee, (4), I rend, 1985; WUS 1, Western United States, (2), Doe]] and Cox, 1972; SV, Sonoma Volcanics, California, (5), Mankinen, 1989.

TABLE 3. Flattening and Rotations, Taos Plateau Volcanic Field

LOCATION	N	I	D	a_{95}	F	dF	R	dR
TPVF MEAN	55	49.3	356.7	3.6	4.1	4.1	-0.6	5.6
NTPVF	18	53.8	357.9	6.8	-0.4	6.2	0.6	9.8
MTPVF	18	49.2	356.5	6.8	4.2	6.2	-0.3	9.0
STPVF	19	45.1	355.9	5.5	8.3	5.3	-1.4	7.2
ETPVF	32	47.7	356.9	4.4	5.7	4.6	-0.4	6.2
WTPVF	23	51.5	356.4	6.3	1.9	5.8	-0.9	8.8
EXPECTED		53.4	357.3	3.5				

NTPVF, MTPVF, STPVF, ETPVF, and WTPVF are collations of sites in this study subdivided into north, middle and south, and again into east and west on geographic location; F and R, flattening and rotation with respect to the expected direction; dF and dR, errors corresponding to F and R calculated using equations in W-own and Golombek (1985) with error corrections as in Demarest (1983).

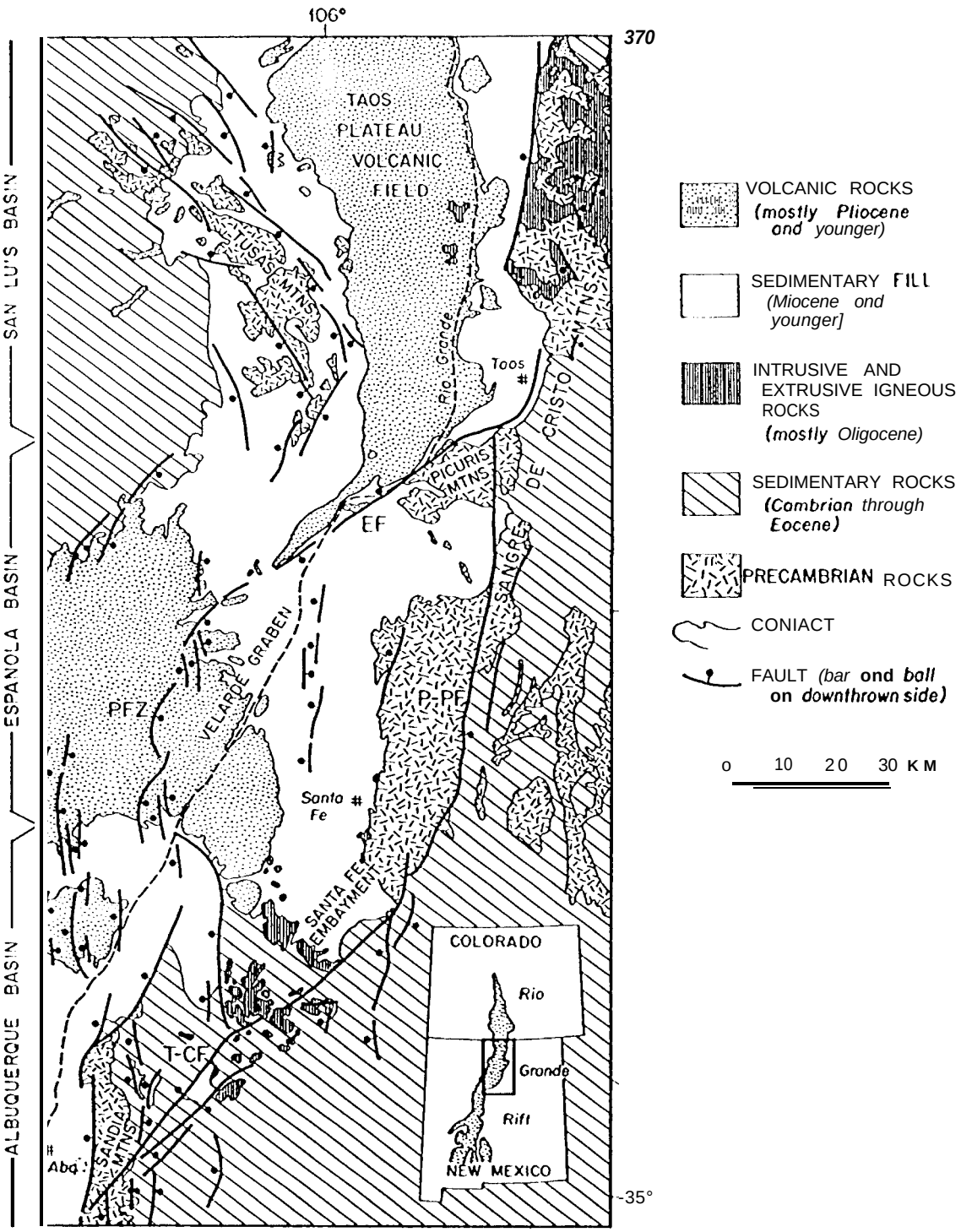
106°
370
35°
SAN LUIS BASIN
ESPANOLA BASIN
ALBUQUERQUE BASIN
TAOS PLATEAU VOLCANIC FIELD
TUSAS MTNS
Rio Grande
Taos
PICURIS MTNS
SANGRE DE CRISTO MTNS
EF
VELARDE GRABEN
PFZ
P-PF
Santa Fe
SANTA FE EMBAYMENT
T-CF
SANDIA MTNS
Abq
COLORADO
Rio
Grande
Rift
NEW MEXICO
VOLCANIC ROCKS (mostly Pliocene and younger)
SEDIMENTARY FILL (Miocene and younger)
INTRUSIVE AND EXTRUSIVE IGNEOUS ROCKS (mostly Oligocene)
SEDIMENTARY ROCKS (Cambrian through Eocene)
PRECAMBRIAN ROCKS
CONIACT
FAULT (bar and ball on downthrown side)
0 10 20 30 KM

Fig. 1

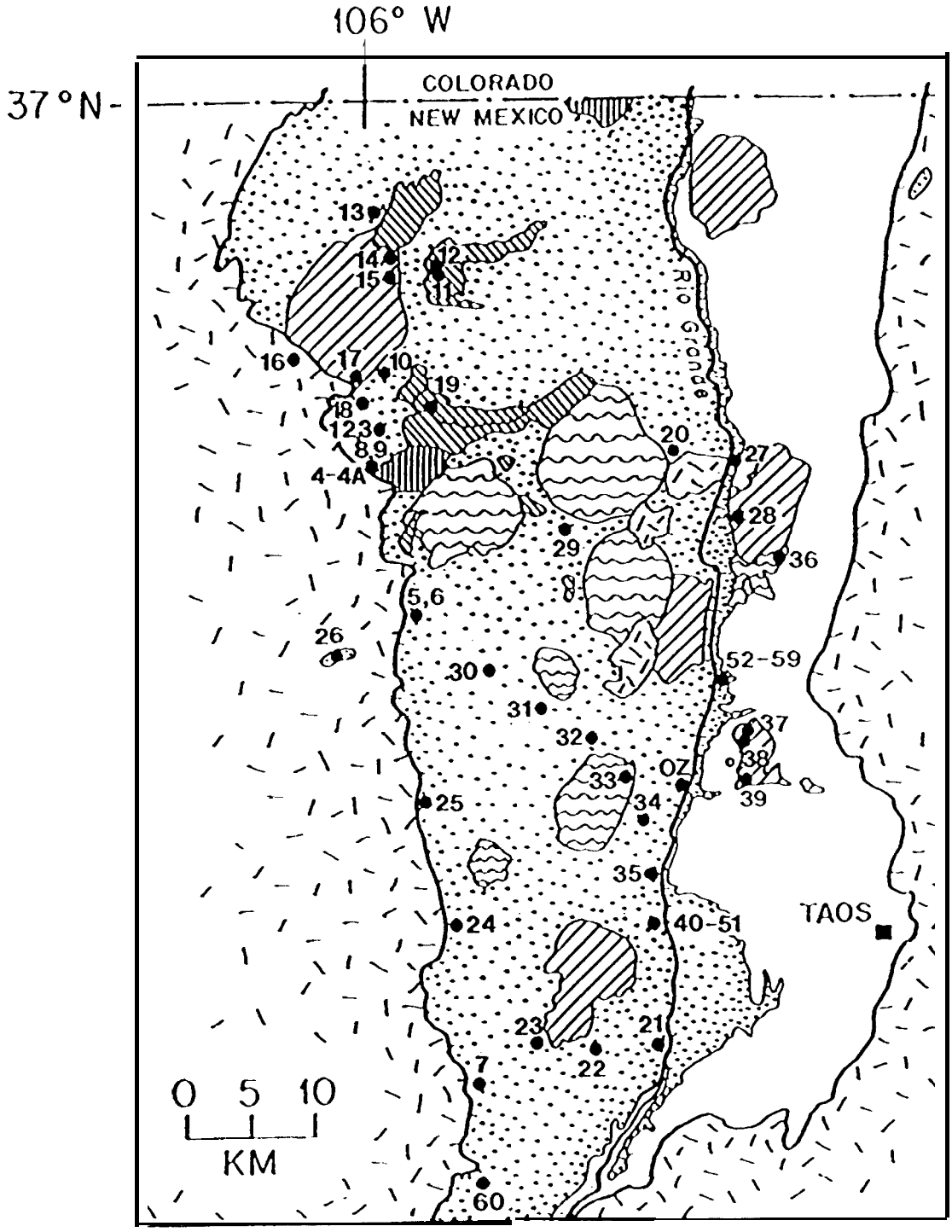
106° W
37°N
COLORADO
NEW MEXICO
Rio Grande
TAOS
0 5 10
KM
13
14
15
12
11
16
17
10
19
18
1
2
3
8,9
4-4A
20
27
28
29
36
5,6
26
30
52-59
31
32
37
38
33
OZ
39
25
34
35
24
40-51
23
21
22
7
60

Fig 2

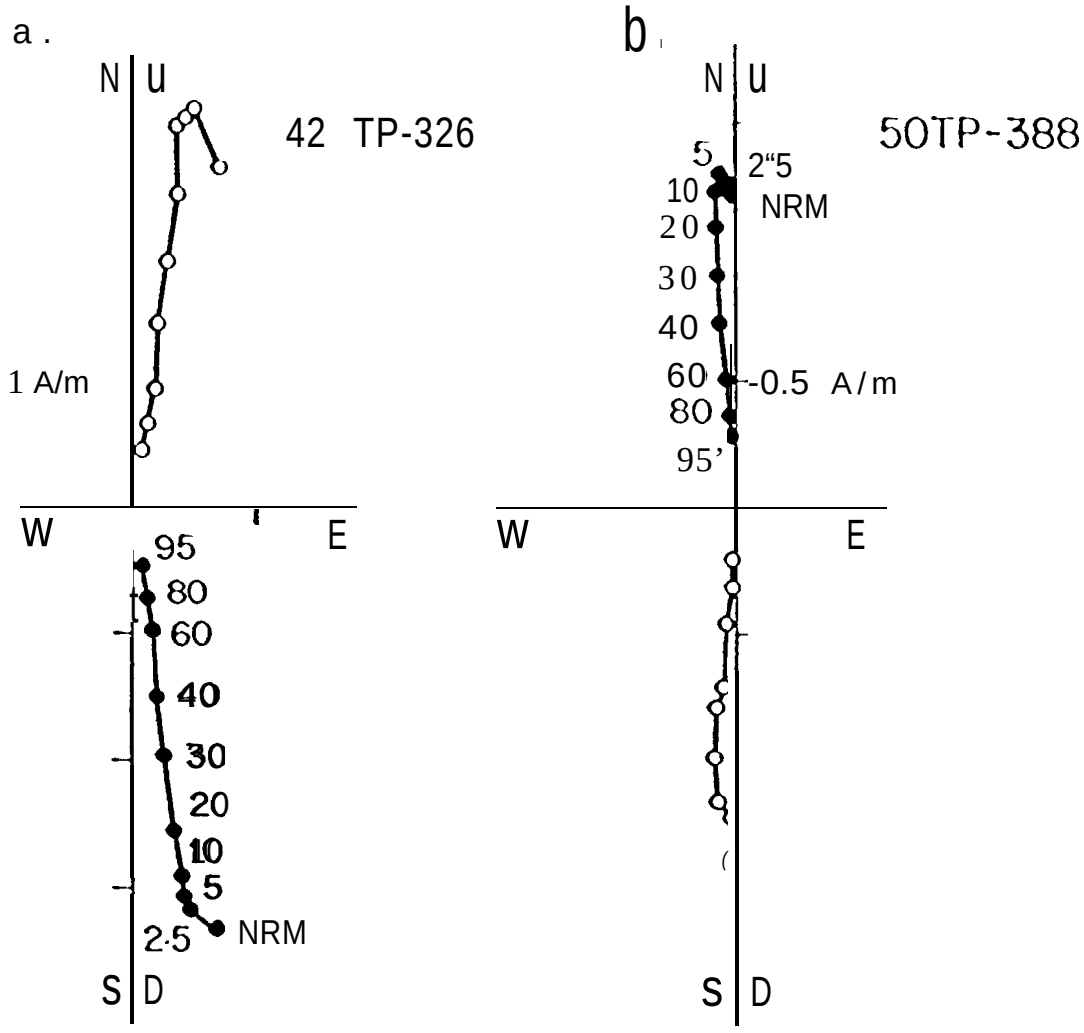
a .
N
U
42 TP-326
1 A/m
W
E
95
80
60
40
30
20
10
5
2.5
NRM
S
D
b
N
U
50TP-388
5
2"5
10
NRM
20
30
40
60
-0.5 A/m
80
95'
W
E
S
D

Fig. 3

c1.

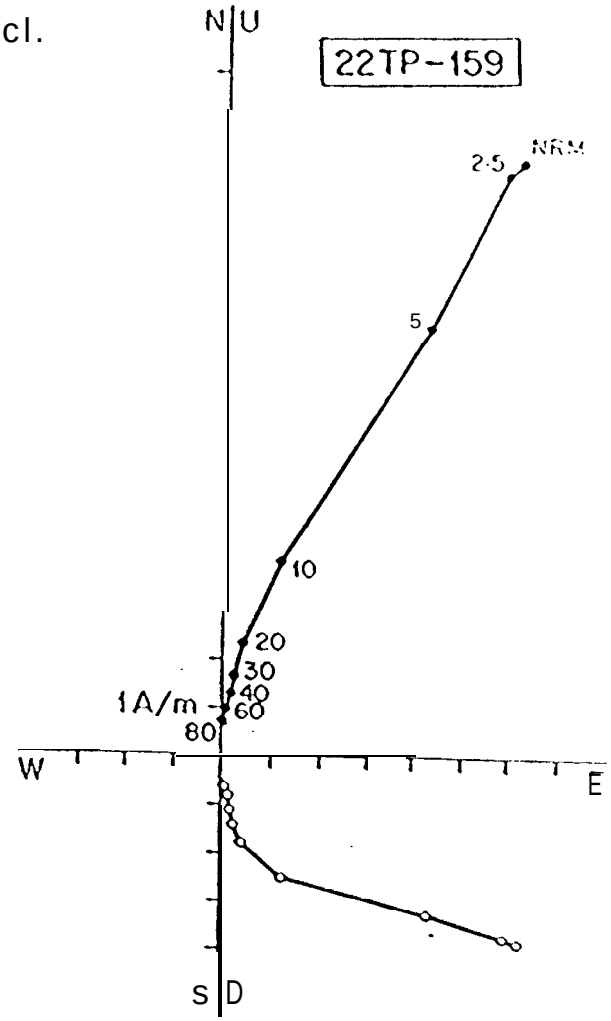
N
U
22TP-159
NRM
2·5
5
10
20
30
40
60
80
1A/m
W
E
S
D

b.

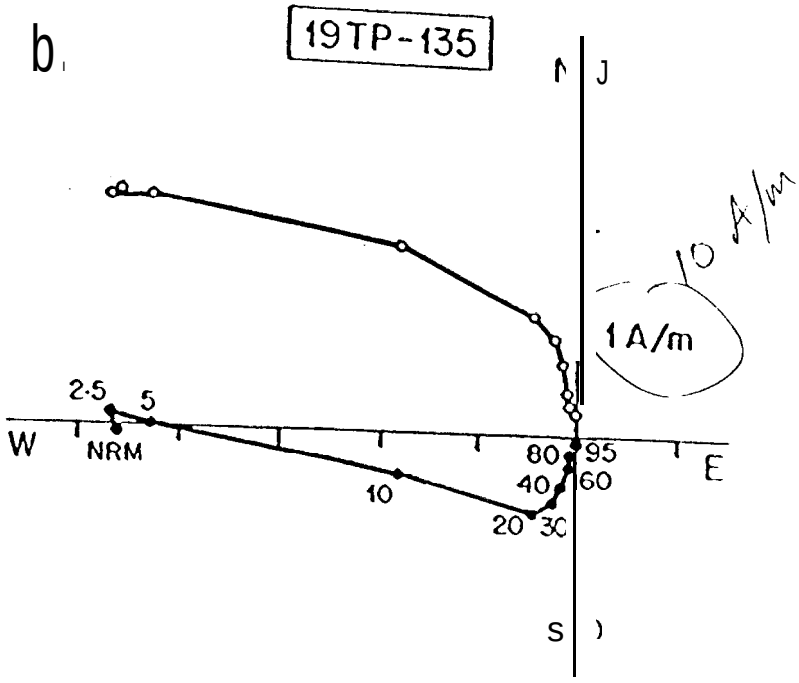
19TP-135
N
J
10 A/m
1A/m
2·5
5
W
NRM
80
95
E
40
60
10
20
30
S

Fig. 4

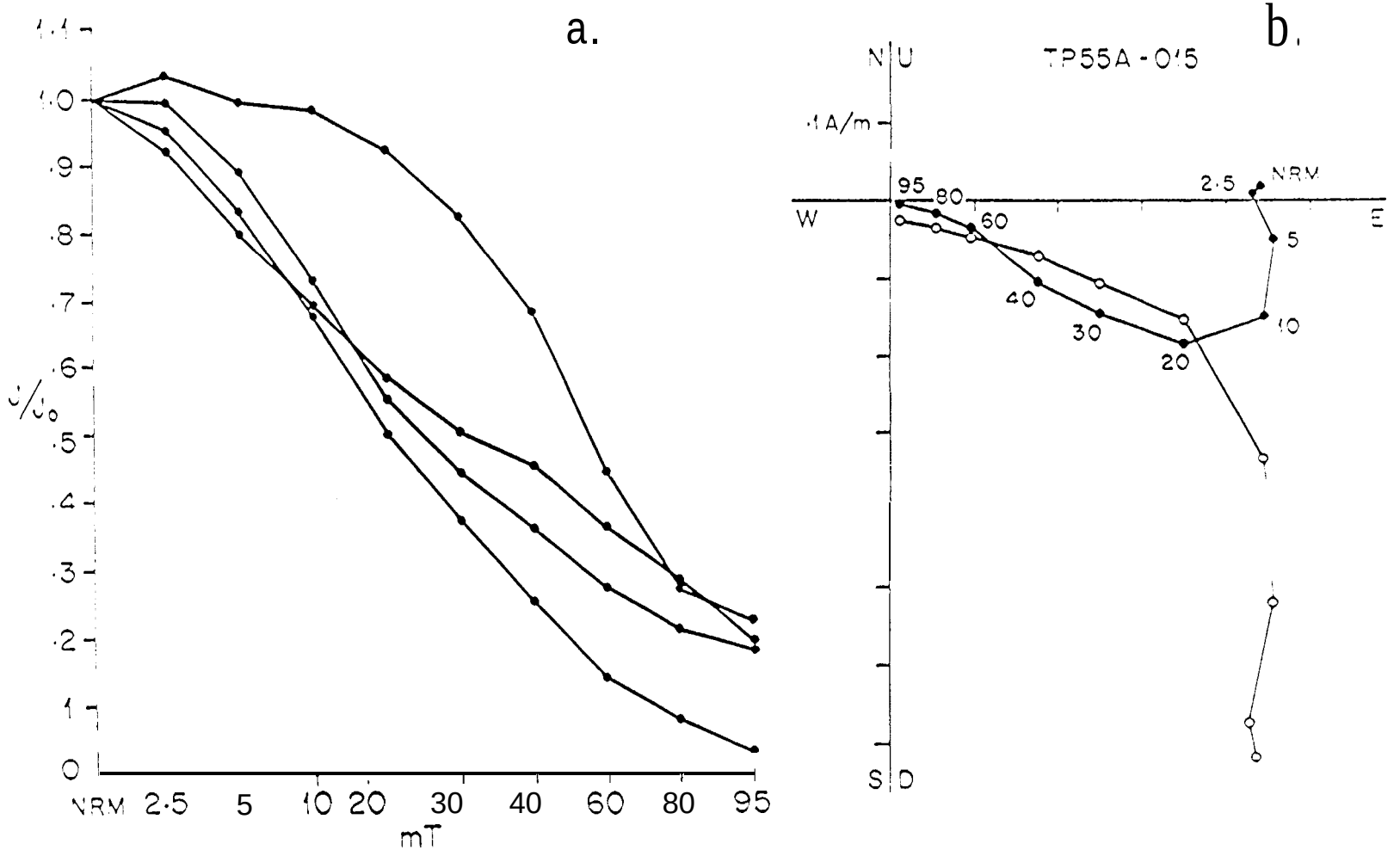
a.
b.
TP55A-015
N|U
·1 A/m
W
E
S|D
NRM
2.5
5
10
20
30
40
60
80
95
J/J₀
1.1
1.0
.9
.8
.7
.6
.5
.4
.3
.2
1
0
NRM 2.5 5 10 20 30 40 60 80 95
mT

Fig. 5

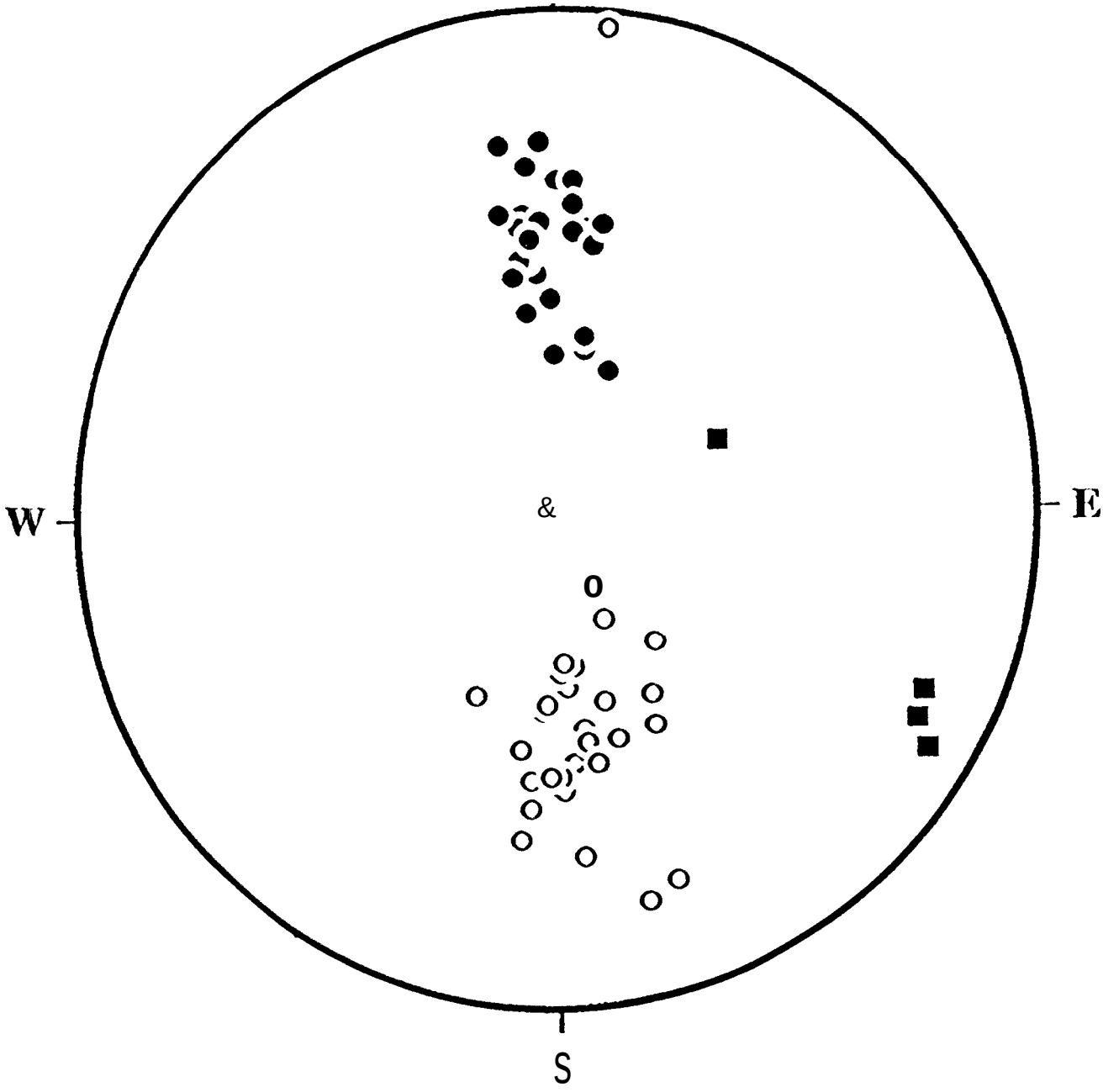

Fig. 6

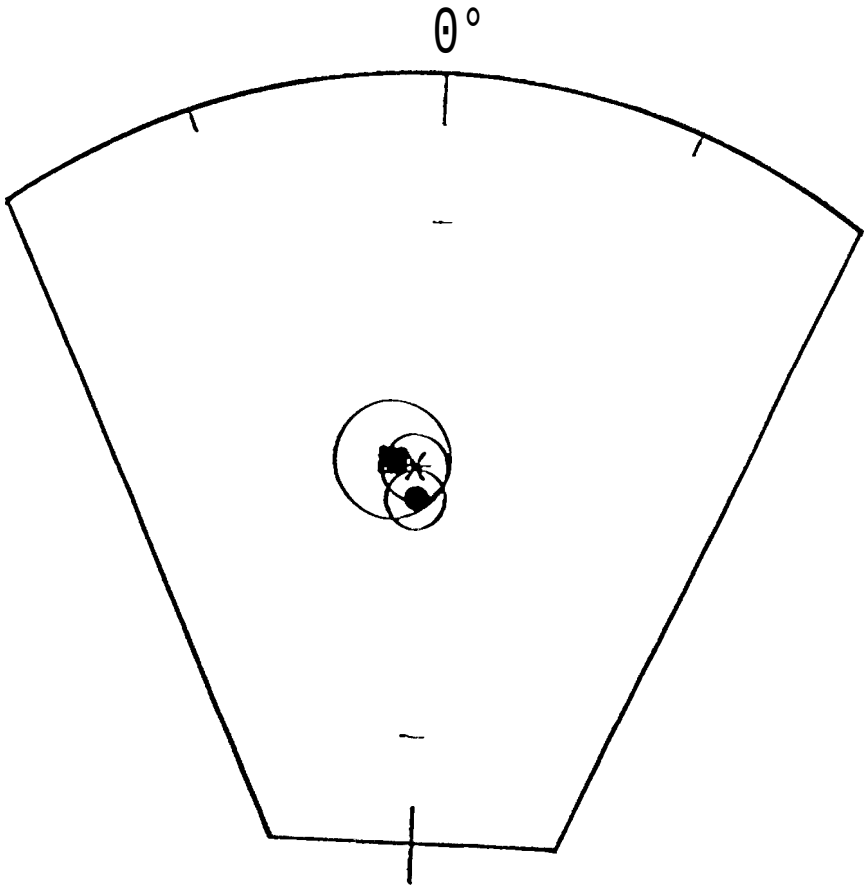

Fig 1

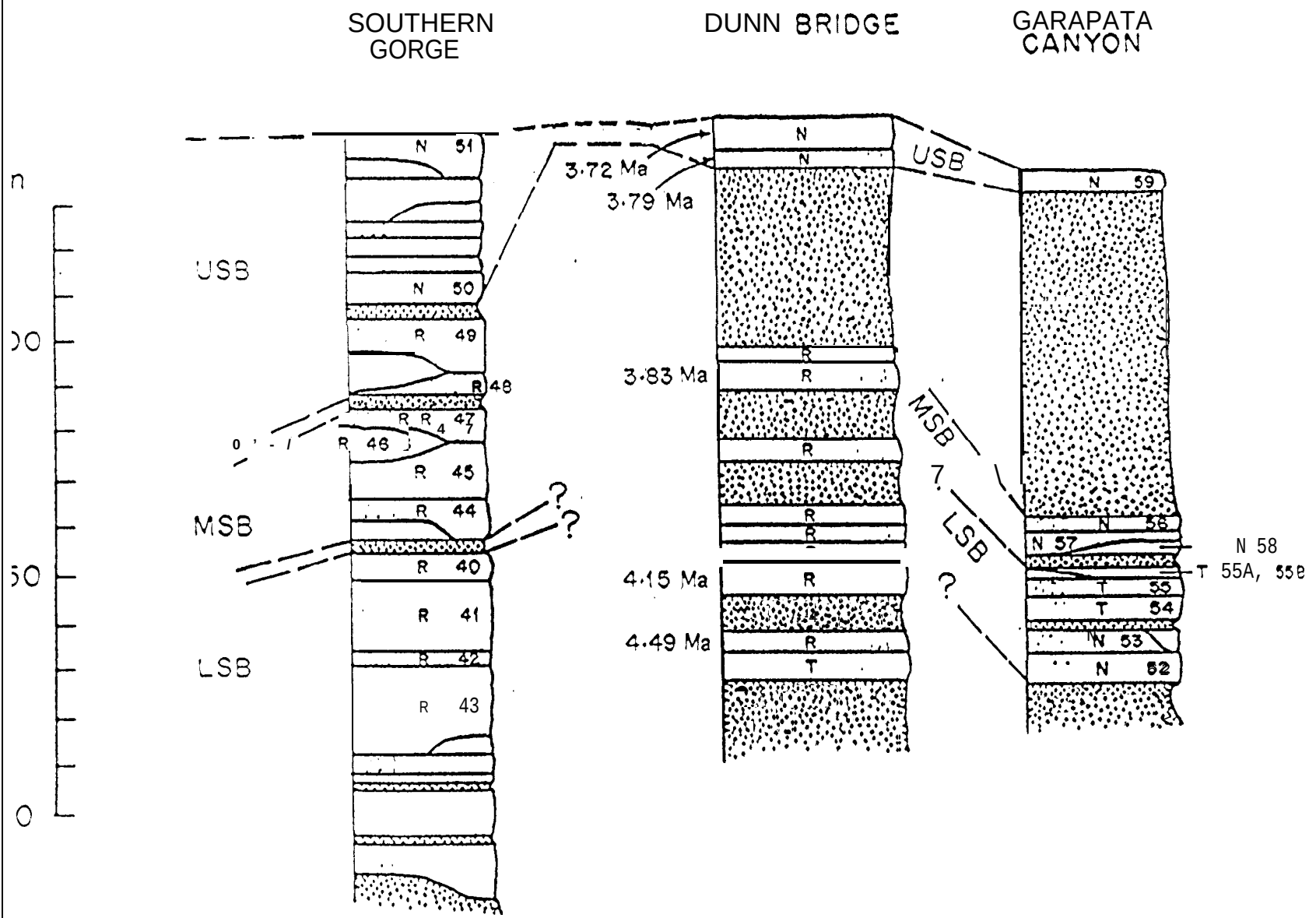
SOUTHERN GORGE
DUNN BRIDGE
GARAPATA CANYON
USB
MSB
LSB
3.72 Ma
3.79 Ma
3.83 Ma
4.15 Ma
4.49 Ma
N 51
N 50
R 49
R 48
R 47
R 46
R 45
R 44
R 40
R 41
R 42
R 43
N 59
N 58
N 57
T 55A, 55B
T 55
T 54
N 53
N 52
?
?
?
n
00
50
0

Fig. 8

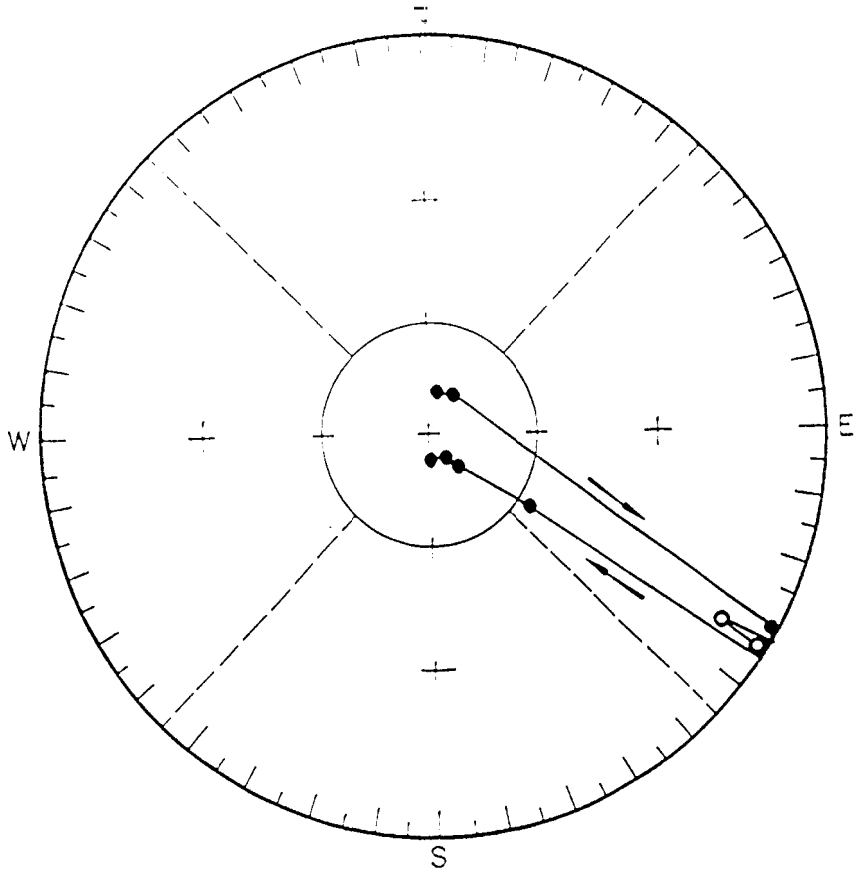

a

b

Fig 9

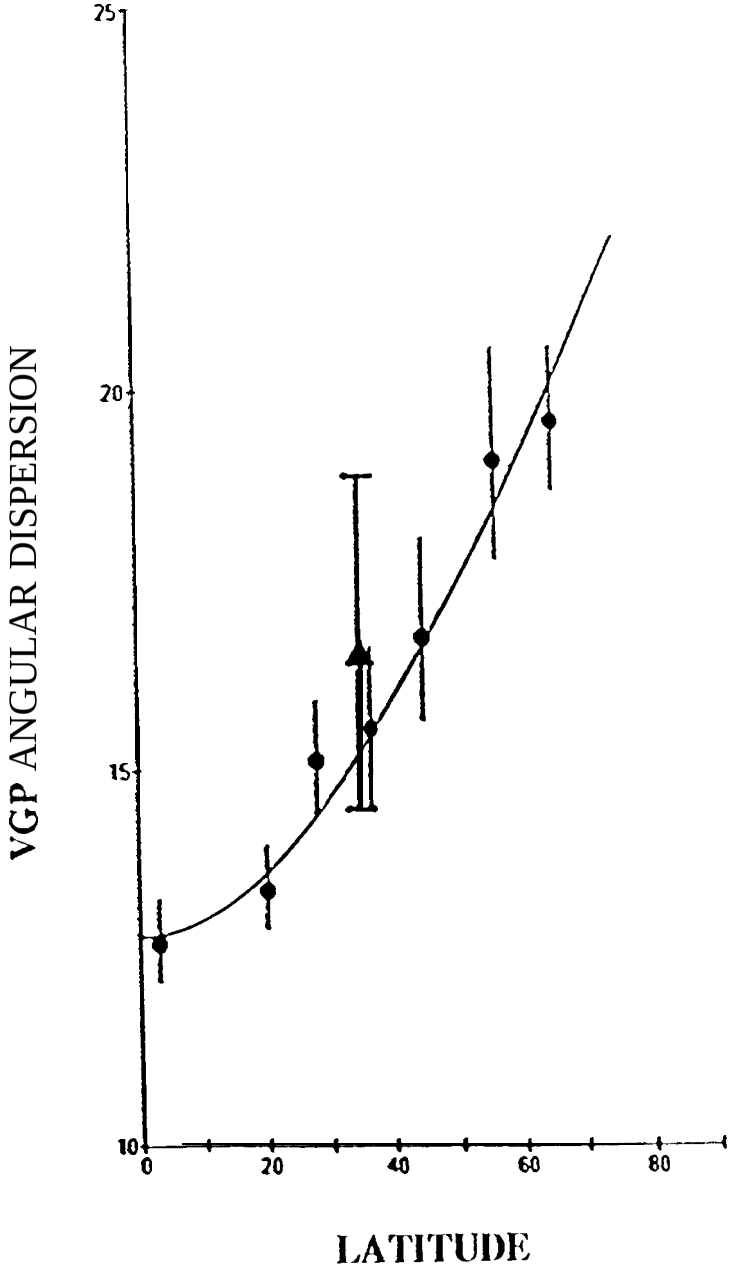

Fig 10

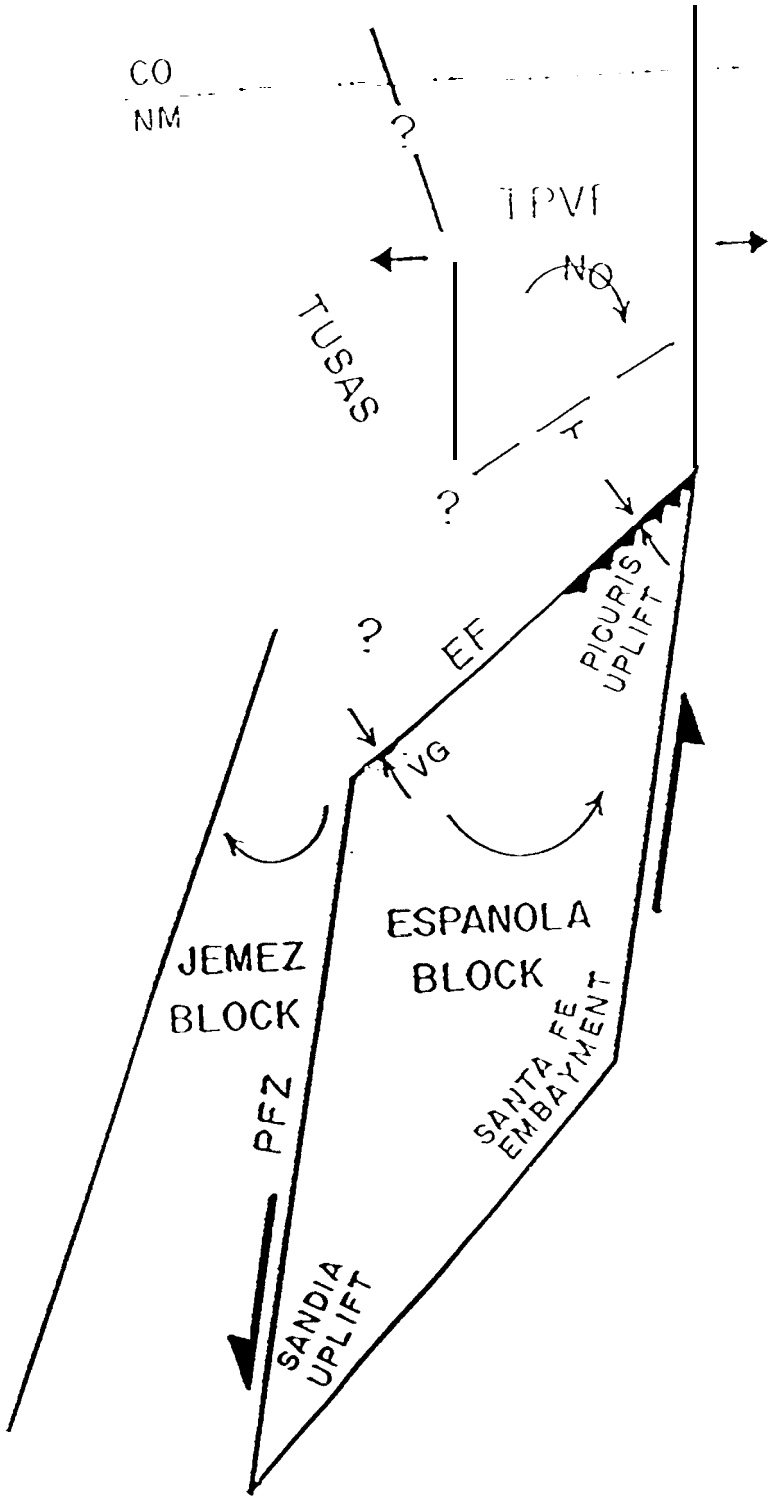
CO
NM
?
TPVF
NO
TUSAS
?
?
EF
PICURIS UPLIFT
VG
JEMEZ BLOCK
ESPANOLA BLOCK
SANTA FE EMBAYMENT
PFZ
SANDIA UPLIFT

Fig. 11